INFECTION AND IMMUNITY, June 2007, p. 2689–2698 Vol. 75, No. 6
0019-9567/07/$08.00+0 doi:10.1128/IAI.01875-06

Murine Aerosol Challenge Model of Anthrax▽

Crystal L. Loving,[1] Mary Kennett,[2] Gloria M. Lee,[1] Vanessa K. Grippe,[1] and Tod J. Merkel[1]*

Laboratory of Respiratory and Special Pathogens, Center for Biologics Evaluation and Research, Food and Drug Administration, 8800 Rockville Pike, Bethesda, Maryland 20892,[1] and Department of Veterinary and Biomedical Sciences, The Pennsylvania State University, State College, Pennysylvania[2]

Received 28 November 2006/Returned for modification 14 February 2007/Accepted 28 February 2007

The availability of relevant and useful animal models is critical for progress in the development of effective vaccines and therapeutics. The infection of rabbits and non-human primates with fully virulent *Bacillus anthracis* spores provides two excellent models of anthrax disease. However, the high cost of procuring and housing these animals and the specialized facilities required to deliver fully virulent spores limit their practical use in early stages of product development. Conversely, the small size and low cost associated with using mice makes this animal model more practical for conducting experiments in which large numbers of animals are required. In addition, the availability of knockout strains and well-characterized immunological reagents makes it possible to perform studies in mice that cannot be performed easily in other species. Although we, along with others, have used the mouse aerosol challenge model to examine the outcome of *B. anthracis* infection, a detailed characterization of the disease is lacking. The current study utilizes a murine aerosol challenge model to investigate disease progression, innate cytokine responses, and histological changes during the course of anthrax after challenge with aerosolized spores. Our results show that anthrax disease progression in a complement-deficient mouse after challenge with aerosolized Sterne spores is similar to that described for other species, including rabbits and non-human primates, challenged with fully virulent *B. anthracis*. Thus, the murine aerosol challenge model is both useful and relevant and provides a means to further investigate the host response and mechanisms of *B. anthracis* pathogenesis.

Bacillus anthracis, the etiological agent of anthrax, is a gram-positive, aerobic, spore-forming, rod-shaped bacterium (25). Dormant spores are highly resistant to adverse environmental conditions and are able to reestablish vegetative growth in the presence of favorable environmental conditions (30). Fully virulent strains of *B. anthracis* harbor two large plasmids, pXO1 and pXO2, which carry the genes required for anthrax toxin production and capsule formation, respectively. The roles of these plasmid-encoded factors in pathogenesis have been extensively studied (for a review, see references10, 26, and 30). *B. anthracis* infection can occur through the skin, the gastrointestinal tract, or through the respiratory epithelium following inhalation of airborne spores and results in cutaneous, gastrointestinal, or inhalational anthrax, respectively (11, 24, 27, 43). The inhalational form of anthrax is the most severe, often associated with rapid progression of disease and death (2, 12, 51). Upon inhalation, anthrax spores reach the bronchioles and alveoli of the lung, where phagocytosis by pulmonary antigen-presenting cells (APCs), such as alveolar macrophages or dendritic cells occurs (4, 6, 16, 18, 38, 40). Following spore uptake, pulmonary APCs are thought to transport *B. anthracis* to the regional lymph nodes. Spores germinate and multiply within the cell, eventually resulting in cell death by lysis (6, 16–18, 22). Vegetative cells multiply within the mediastinal lymph node and gain entry into the bloodstream, resulting in the development of severe bacteremia (28, 38). Disease progression leads to vascular injury with edema, hemorrhage, and thrombosis, ultimately resulting in the death of the host (5).

The availability of relevant and useful animal models is critical for advances in our understanding of *B. anthracis* pathogenesis and for progress in the development of effective vaccines and therapeutics directed against *B. anthracis*. Although rabbits and non-human primates infected with fully virulent *B. anthracis* spores provide two excellent models of disease, the high cost of procuring and housing these animals, as well as the specialized facilities required to deliver fully virulent aerosolized spores, limits the practical use of these animals in basic research laboratories. The small size and low cost associated with mice makes the murine model more practical for conducting experiments in which large numbers of animals are required for challenge. In addition, the ability to manipulate the genetics of the challenge species (transgenic and knockout strains) and the availability of well-characterized immunological reagents make it possible to perform studies in mice that could not be easily performed in other species. Finally, the ability to use the attenuated, capsule-negative strain of anthrax in the mouse model greatly facilitates the ability of researchers in the anthrax field to use this animal model for their studies without the biocontainment concerns associated with fully virulent strains.

The lethality of nontoxigenic, encapsulated ($pXO1^-$ $pXO2^+$) strains of anthrax in mice and the failure of protective antigen-based vaccines to protect mice after challenge with virulent strains of *B. anthracis* spores have led to the perception that the mouse model does not accurately reflect the disease observed in humans (47). It is important to note that the lethality with $pX02^+$ strains has been clearly linked to the expression of capsule and can be avoided by using the capsule-

* Corresponding author. Mailing address: Laboratory of Respiratory and Special Pathogens, DBPAP/CBER/FDA, Building 29, Room 418, 29 Lincoln Drive, Bethesda, MD 20892. Phone: (301) 496-5564. Fax: (301) 402-2776. E-mail: merkel@cber.fda.gov.

▽ Published ahead of print on 12 March 2007.

negative Sterne strain ($pX02^-$) (48). Particular strains of mice, such as C57BL/6 and BALB/c, are resistant to challenge with nonencapsulated strains of *B. anthracis*; however, complement-deficient mice, such as A/J mice or cobra venom factor-treated C57BL/6 mice, are sensitive to aerosol challenge with nonencapsulated Sterne spores (20, 48). In the current study, we have characterized the outcome of aerosol infection of A/J mice with spores prepared from *B. anthracis* strain 7702 ($pX01^+$ $pX02^-$) and report that when complement-deficient mice are exposed to aerosolized spores of the capsule-negative Sterne strain, the resulting disease recapitulates the pathology observed in rabbits and non-human primates challenged with the fully virulent strain. We have used the model to begin to investigate the in vivo innate immune response after aerosol challenge with spores. Overall, our results indicate that the mouse aerosol challenge model is a useful and relevant model of *B. anthracis* infection that can be used to further elucidate the mechanisms of *B. anthracis* pathogenesis as well as provide a means in which to screen potential anthrax vaccines and therapeutics.

MATERIALS AND METHODS

Aerosol challenge of A/J mice. Male and female A/J mice were purchased from Jackson Laboratory (Bar Harbor, ME) and maintained at the Center for Biologics Evaluation and Research. Mice were challenged between 6 and 12 weeks of age, as previously described (34). Briefly, mice were exposed to aerosolized spores for 90 min using a nose-only exposure system (CH Technologies, Westwood, NJ). Mice were supplied with fresh air for 10 min before and after the exposure to spores. The spore inoculum for each challenge, prepared from *B. anthracis* strain 7702, contained 15 ml of 5×10^9 spores/ml in distilled H_20 with 0.01% Tween 80. Generation and purification of spores were carried out as previously described (8, 33). Immediately following challenge four mice per challenge group were euthanized, and their lungs were homogenized, serially diluted, and plated to determine the average number of spores retained, reported as the number of CFU. Mice were retained for survival or euthanized at various times postchallenge for tissue collection. All mice were housed and maintained at the Center for Biologics Evaluation and Research animal facility under the approval of the Institutional Animal Care and Use Committee.

Bacterial dissemination. To measure bacterial dissemination, mice were euthanized at various times postchallenge, and the lungs, liver, spleen, and draining lymph nodes (hilal and mediastinal) were collected. Tissues were homogenized in phosphate-buffered saline, serially diluted, and plated on brain heart infusion agar to determine numbers of CFU. In order to distinguish between spores and bacilli, a fraction of each tissue homogenate was heat treated at 65°C for 30 min to kill any bacilli. Heat-treated and untreated samples were serially diluted and plated, and results were recorded as numbers of CFU. Each figure distinguishes between untreated and heat-treated samples for discerning the number of spores plus bacilli (untreated) versus the number spores alone (heat treated). The limits of detection were 250 CFU for lungs, liver, and spleen and 10 CFU for lymph nodes.

Histopathology. Mice were euthanized at the time points postinfection indicated in the figure legends, and the spleen, liver, heart, and lungs (inflated with formalin) were fixed in neutral buffered formalin. Tissue sections were routinely prepared and stained with hematoxylin and eosin at the Pennsylvania State University Animal Diagnostic Laboratory. Sections were examined by light microscopy by a veterinarian with training and experience in rodent pathology (M. J. Kennett). Representative sections were photographed using a Nikon Digital Camera DMX1200F.

Tissue harvesting for cytokine analysis. Lungs, liver, and lymph nodes were homogenized in a buffer (14) that contained 0.5% Triton X-100, 150 mM NaCl, 15 mM Tris, 1 mM $CaCl_2$, and 1 mM $MgCl_2$, pH 7.4. Protease inhibitors were added per the manufacturer's instructions (Complete EDTA-free; Roche Diagnostics, Indianapolis, IN). Tissues from three animals were routinely pooled to generate single samples in order to accommodate the small size of lymph nodes. Lungs and 300 mg of liver were homogenized in 2.5 ml of buffer using a Stomacher (Sewar, Inc., Thetford, Norfold, United Kingdom), and lymph nodes were homogenized in 300 μl using a pellet pestle (Kontes Glass Co., Vineland, NJ). Samples were incubated at 4°C for 30 min after homogenization. Lung and liver supernatants were passed over a 40-μm-pore-size filter (BD Biosciences, Bedford, MA). Lymph node samples were centrifuged at 10,000 × *g* for 10 min at 4°C, and the supernatant was collected. All samples were stored at −80°C for later assessment of cytokine levels.

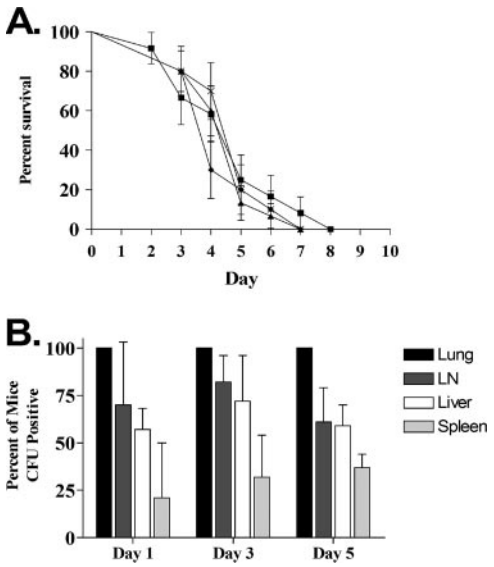

FIG. 1. Survival and bacterial dissemination after aerosol challenge of A/J mice. Groups of mice were exposed to aerosols of *B. anthracis* spores (strain 7702) and observed for survival (A) or bacterial dissemination (B) on days 1, 3, and 5 postchallenge. The actual dose retained in the lungs of animals following exposure was determined for a subset of mice from each challenge. Doses of 2.7×10^6 (squares), 2.4×10^6 (circles), and 2.25×10^6 (x) spores were delivered. Dissemination is reported as the percentage of mice positive for CFU in lung, lymph node (LN), liver, or spleen on day 1, 3, or 5 postchallenge.

Cytokine analysis. Lung, liver, and lymph node homogenates were thawed on ice and centrifuged at 300 × *g* for 5 min to pellet any cellular debris. Tumor necrosis factor alpha (TNF-α) cytokine levels were determined using a commercially available enzyme-linked immunosorbent assay (ELISA) kit (Biosource, Carlsbad, CA) according to the manufacturer's recommendations. A student's *t* test was used for statistical analysis, and *P* values of <0.05 are indicated.

RESULTS

Aerosol challenge of mice. A number of murine challenge models of anthrax have been described that utilize different routes of administration of *B. anthracis* spores. These include intraperitoneal injection, subcutaneous injection, intranasal instillation (i.n.), and intratracheal instillation (i.t.). For the study of inhalational anthrax, the model that best recapitulates the natural route of infection is the aerosol challenge model. Although the mouse aerosol challenge model has been used to examine the outcome of *B. anthracis* infections, a detailed characterization of the infection in mice after challenge with aerosolized *B. anthracis* spores is lacking. To determine the 50% lethal dose (LD_{50}) of *B. anthracis* strain 7702 spores delivered to A/J mice by the aerosol route, groups of 10 mice were challenged with retained doses between 1×10^3 and 1×10^6 spores per mouse, and the LD_{50} was calculated by the method of Reed and Muench (36). In three independent experiments, LD_{50} values of 7×10^4, 1.4×10^5, and 3×10^5 were calculated, yielding an average LD_{50} of 2×10^5 spores per mouse. When a dose of approximately 20 times the calculated LD_{50} (4×10^6) was delivered in three independent aerosol

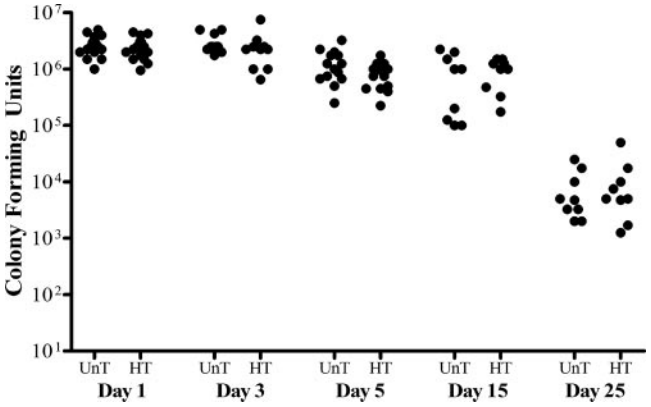

FIG. 2. Bacilli and spore loads in the lungs of mice challenged with aerosolized *B. anthracis* Sterne spores. Groups of A/J mice were exposed to aerosols of spores with an average pulmonary retained dose of 3×10^6 spores per mouse, and the number of CFU in the lungs of surviving mice was measured at days 1, 3, 5, 15, and 25 postchallenge. Germination gives rise to heat-sensitive vegetative bacilli and would be indicated by a reduction in the number of CFU in heat-treated (HT) versus untreated (UnT) samples. Therefore, a fraction of each lung homogenate was heat treated at 60°C for 30 min prior to diluting and plating. UnT CFU values are for spores and bacilli, HT CFU values are spores only.

challenges, the mean time to death across all three challenges was 4.7 ± 1.6 days (Fig. 1A). Although the majority of deaths occurred on days 4, 5, and 6, death occurred as early as day 2 and as late as day 8. Death before day 2 or after day 10 was never observed. Mice remained asymptomatic until approximately 12 to 24 h prior to death, at which time, symptoms such as piloerection; edematous swelling of the chest, neck, or head; hind-limb paralysis; and lethargy became apparent.

Dissemination of infection. In order to characterize the dissemination of infection following aerosol exposure of A/J mice to *B. anthracis* strain 7702 spores, groups of mice were challenged at a level which achieved pulmonary retained doses of 2×10^6 to 4×10^6 spores. On days 1, 3, and 5 postchallenge, mice were sacrificed, and the numbers of CFU in lungs, draining lymph nodes, spleen, and liver were determined. Dissemination was assessed by scoring individual tissue samples from each challenged animal for the presence of *B. anthracis*, without regard to the number of CFU per tissue. As expected, 100% of challenged mice were positive for *B. anthracis* in the lungs on all days examined (Fig. 1B). As early as day 1 postchallenge, CFU were detected in the draining lymph nodes of 70% of mice and in the livers of nearly 60% of mice. Interestingly, only 21% of spleens from mice euthanized day 1 postchallenge were positive for CFU (Fig. 1B). The values reported for days 3 and 5 postchallenge were slightly higher for each tissue, but the overall pattern remained the same. These results demonstrate that following aerosol challenge of A/J mice with Sterne strain spores, dissemination to distal organs can occur as early as 1 day after challenge. Significantly, regardless of the day postchallenge, some percentage of mice was observed with no signs of disseminated disease.

We next analyzed the same set of data and considered the number of CFU per tissue (Fig. 2 and 3). As expected, the

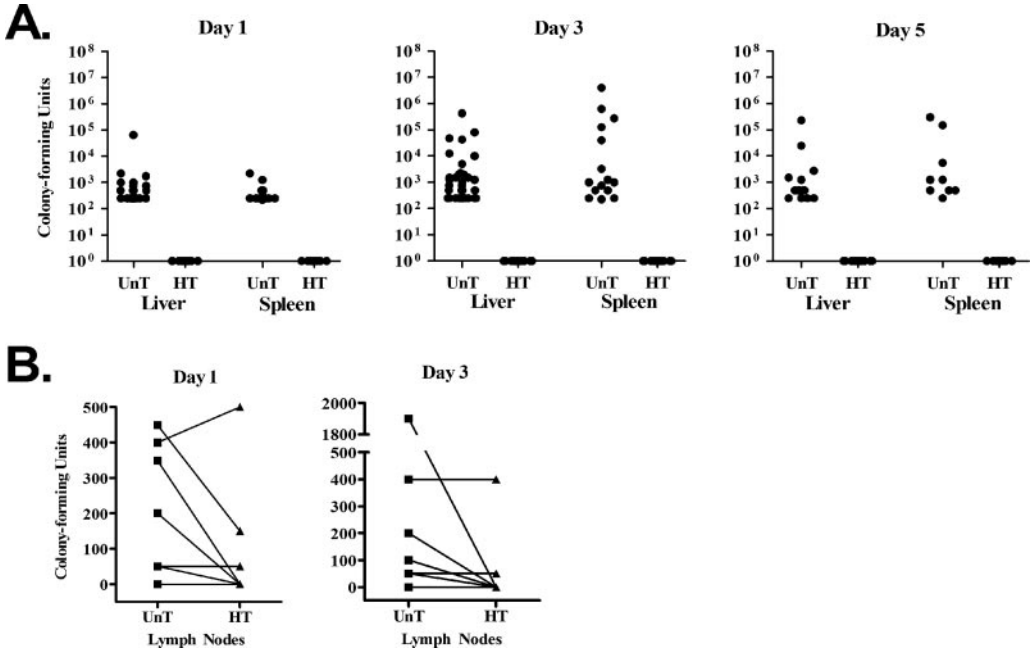

FIG. 3. Bacilli and spore load in distal organs of mice challenged with aerosolized *B. anthracis* Sterne spores. Groups of A/J mice were exposed to aerosols of spores with an average pulmonary retained dose of 3×10^6 spores per mouse. The numbers of CFU in the liver and spleen (A) and pulmonary draining lymph nodes (hilal and mediastinal) (B) were measured on days 1, 3, and 5 postchallenge. Germination of spores gives rise to heat-sensitive bacilli. To determine CFU resulting from spores or spores plus bacilli, a fraction of each homogenate was heat treated (HT) at 60°C for 30 min prior to diluting and plating. Untreated (UnT) CFU values are for spores and bacilli, whereas HT CFU values are spores only. Counts for the liver represent CFU in 300 mg of tissue and counts for the spleen represent total organ CFU. Counts for lymph nodes are CFU/ml of tissue homogenate. The limits of detection were 250 CFU for the liver and spleen and 10 CFU for the lymph nodes.

number of CFU in the lungs of challenged mice 1 day postchallenge (~2.75×10^6 spores) was within the initially targeted retained dose of 2×10^6 to 4×10^6 spores per mouse. The CFU values in the lungs on day 3 were similar to the value observed on day 1 (3×10^6) with a slight decrease observed at day 5 (1.3×10^6). To determine whether or not spores germinated in the lung, a fraction of each lung homogenate was heat treated to kill any vegetative cells prior to plating. Germination gives rise to heat-sensitive vegetative cells and would be indicated by reduced numbers of CFU in heat-treated samples relative to untreated samples. On days 1, 3, and 5 no significant differences were observed between the lung CFU values in heat-treated relative to the untreated homogenates (Fig. 2), which indicates a lack of germination in the lungs of infected mice at early time points postchallenge. Histological examination of the lungs 5 days after spore challenge showed minimal inflammatory responses and a lack of bacilli in lung tissue (Fig. 4), which is in accordance with the results from lung CFU (Fig. 2).

In order to determine if germination in the lungs occurred at later times after infection, we retained any mice that survived aerosol challenge beyond day 10. By alternatively distributing the rare survivors from a large number of challenges into two groups, we were able to accumulate a large sample of mice in each group ($n = 18$). The mice in one group were sacrificed on day 15 postchallenge ($n = 9$), and the mice in the second group were sacrificed on day 25 postchallenge ($n = 9$). There was no difference in the numbers of CFU in the untreated and heat-treated lung homogenates, even 15 and 25 days postchallenge (Fig. 2), indicating the presence of spores but not vegetative bacilli. Although the number of spores in the lungs decreased over time, these results indicate that most, if not all, of the spores in the lung remain dormant.

Unlike the lung, differences were observed in CFU counts after heat treatment of lymph node, liver, and spleen homogenates, which indicates the presence of vegetative bacilli in these tissues (Fig. 3). Although CFU could be detected in the lymph nodes, liver, and spleen of infected animals by day 1 postchallenge, the CFU values in these tissues were low compared to the lung. Interestingly, the lymph nodes contained a mix of heat-sensitive and -insensitive CFU, indicating the likelihood that lymph nodes contain both spores and vegetative bacilli (Fig. 3B). However, CFU counts in the liver and spleen were sensitive to heat treatment at all days examined, indicating the presence of vegetative bacilli but not spores (Fig. 3A). On days 3 and 5 postchallenge a wide range of CFU values for the liver and spleen were measured, ranging from animals with 2.5×10^2 CFU to 5×10^5 CFU, and we hypothesized that this was due to differences in timing of dissemination from the lung between mice. This would explain differences in time to death of animals and the observation that even in challenges with 100% mortality there were some mice without CFU in distal organs on each day examined. In addition, it would explain the variability in CFU counts in the livers and spleens, as animals with no CFU in distal organs were probably animals in which dissemination from the lung had not yet occurred. Distal organs that were only recently seeded would have low CFU values, and organs with high CFU counts were likely animals whose organs had been seeded earlier, thereby permitting a longer period of bacterial replication. If this hypothesis were correct, one would predict that all animals at late stages of disease would have high CFU values in the liver and spleen. To test this possibility, a large number of mice were challenged, and regardless of the day postchallenge, only moribund animals were sacrificed. The numbers of CFU in the lungs, lymph nodes, liver, and spleen were determined as well as the percentage of animals CFU positive in each of these tissues (Fig. 5). As predicted, all moribund animals had high CFU counts in all tissues examined. In addition, lungs of moribund animals likely contained both spores and vegetative bacilli, as heat treatment of lung homogenates from moribund animals resulted in a decrease in CFU values (Fig. 5A).

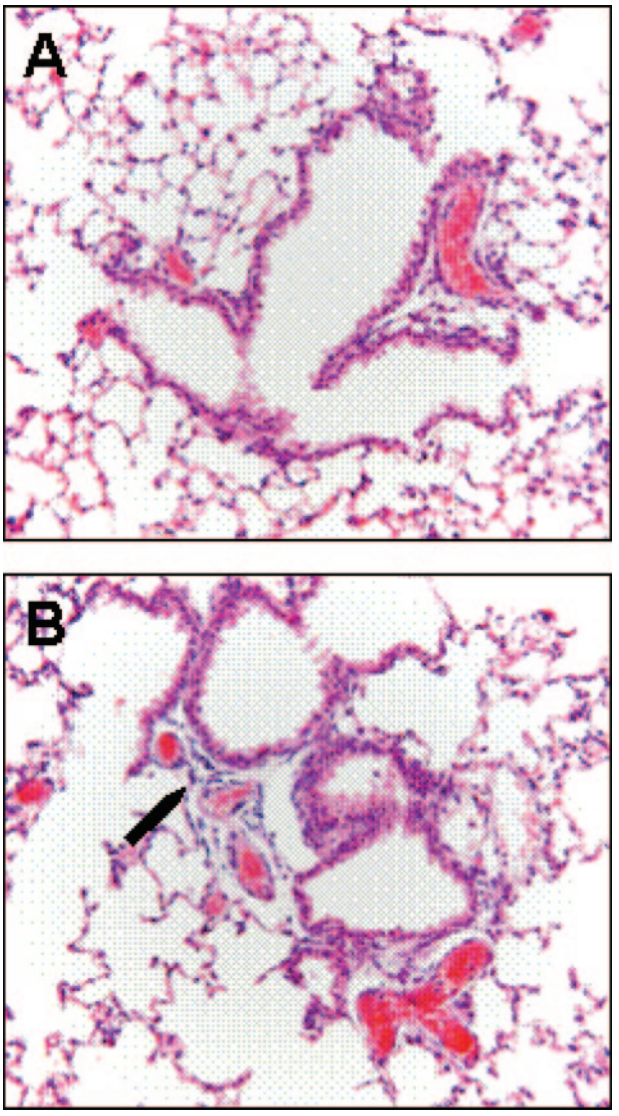

FIG. 4. Representative light photomicrographs of hematoxylin- and eosin-stained lung sections collected from nonchallenged control A/J mice (A) or A/J mice challenged with aerosolized *B. anthracis* Sterne spores 5 days postchallenge (B). The arrow indicates mild lymphocytic response present in challenged mice. Original magnification, ×200.

Histopathology of moribund mice. To compare pathological changes observed in mice to other animal models of inhala-

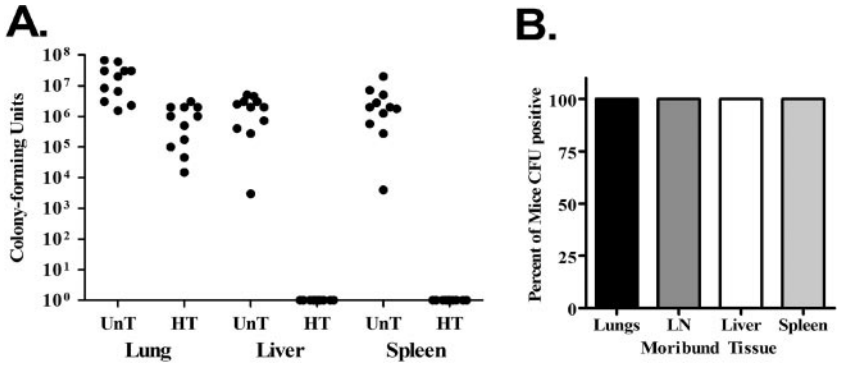

FIG. 5. Bacilli and spore load in lungs and distal organs of moribund mice after aerosol challenge with *B. anthracis*. Groups of A/J mice were exposed to aerosols of spores with an average pulmonary retained dose of 3×10^6 spores per mouse. Upon daily examination, regardless of the day postchallenge, any mouse that appeared moribund (i.e., ruffled fur, hunched over, or shallow breathing) was euthanized and the numbers of CFU in the lung, liver, and spleen (A) and the percentages of moribund mice CFU positive in lung, lymph node (LN), liver, and spleen (B) were determined. To determine CFU resulting from spores or spores plus bacilli (germination gives rise to heat-sensitive bacilli), a fraction of each homogenate was heat treated (HT) prior to diluting and plating. Untreated (UnT) CFU values are for spores and bacilli whereas HT CFU values are for spores only.

tional anthrax, groups of mice were challenged, and the lungs, heart, liver, and spleen were collected from five moribund mice, regardless of the day postchallenge (Fig. 6). In heart tissue, four out of five mice had large clusters of bacilli in the myocardium with mild lymphocytic to no inflammatory response. Splenic lesions ranged from lymphocyte depletion (apoptosis) to areas of hemorrhage. One mouse exhibited widespread necrotizing splenitis with numerous bacterial colonies. In liver tissue, three of five mice had numerous bacteria in liver vessels and sinusoids, while two mice had mild hemorrhages with no bacteria observed, although one animal did have a localized area of necrosis. Lung lesions ranged from none (two of five mice) to bacterial colonies with little inflammatory response (two of five mice) to an animal with extensive hemorrhage, consolidation and necrosis, and numerous bacterial colonies. As a group, three out of five mice had bacterial colonies present in three to four of the tissue types examined; one mouse had a colony in the myocardium, while one mouse showed no visible bacterial colonies in any of the tissues examined.

In vivo cytokine response to *B. anthracis* after aerosol challenge. Various studies have examined the production of cytokines after in vitro stimulation of primary cells with *B. anthracis*, but few reports are available on the cytokine response in vivo after challenge. In order to begin to examine the in vivo cytokine response to inhalational anthrax, homogenates of lungs, lymph nodes, and livers were collected on days 1 and 3 postchallenge and assayed for TNF-α levels. Although all tissues examined showed a significant increase in the amount TNF-α compared to sham-treated animals, the relative increase was significantly different among the three tissue types (Fig. 7). On either day examined, the increase in TNF-α in the lungs was approximately 1.5 times higher than in uninfected animals. The differences in the liver were slightly higher, with an average threefold increase in TNF-α levels after challenge. Interestingly, the lymph nodes showed the greatest increase in TNF-α levels on day 1 after challenge with more than a sevenfold increase in TNF-α levels over sham-treated mice; however, by day 3 this value had decreased, with an approximate threefold increase in TNF-α levels. It is difficult to compare concentrations across the three tissues because each contained a different amount of tissue by weight. Nevertheless, the relative increase over sham-treated animals shows a robust response in the lymph nodes within 1 day of challenge. It was difficult to obtain enough animals to examine levels beyond day 3 postchallenge because of the high mortality rate associated with disease and the large number of animals required to pool lymph node samples.

DISCUSSION

Animal models of human disease play an important role in providing insight to the mechanisms of pathogenic disease. Mice provide a very useful model for studying pulmonary *B. anthracis* pathogenesis because they are relatively inexpensive and easy to maintain and handle. In addition, mice are valuable for studying mechanisms of host defense during infection because of the availability of immunological reagents and knockout strains. For studying *B. anthracis* pathogenesis in mice, it is critical to use a nonencapsulated strain of anthrax because previous research indicates that capsule expression is lethal in mice (21, 46, 50). To circumvent capsule-associated lethality in mice, $pX02^-$ strains of *B. anthracis* have been used, but these nonencapsulated strains are attenuated in many strains of mice (49). Complement-deficient mice, such as A/J mice or cobra venom factor-treated C57BL/6 mice, are sensitive to challenge with *B. anthracis*, regardless of capsule expression (20, 48). The current study outlines the course of inhalational *B. anthracis* disease in A/J mice after exposure to aerosolized Sterne spores, and data indicate that the dissemination and outcome of disease as well as the pathological changes in various organs are similar to other animal models (non-human primates and rabbits) challenged with fully virulent spores. Thus, using complement-deficient mice with a nonencapsulated strain of *B. anthracis* allows for investigating disease pathogenesis without using fully virulent bacterial strains ($pXO1^+$ $pXO2^+$). This makes the murine model used in the current study valuable because disease progression is similar to the progression that

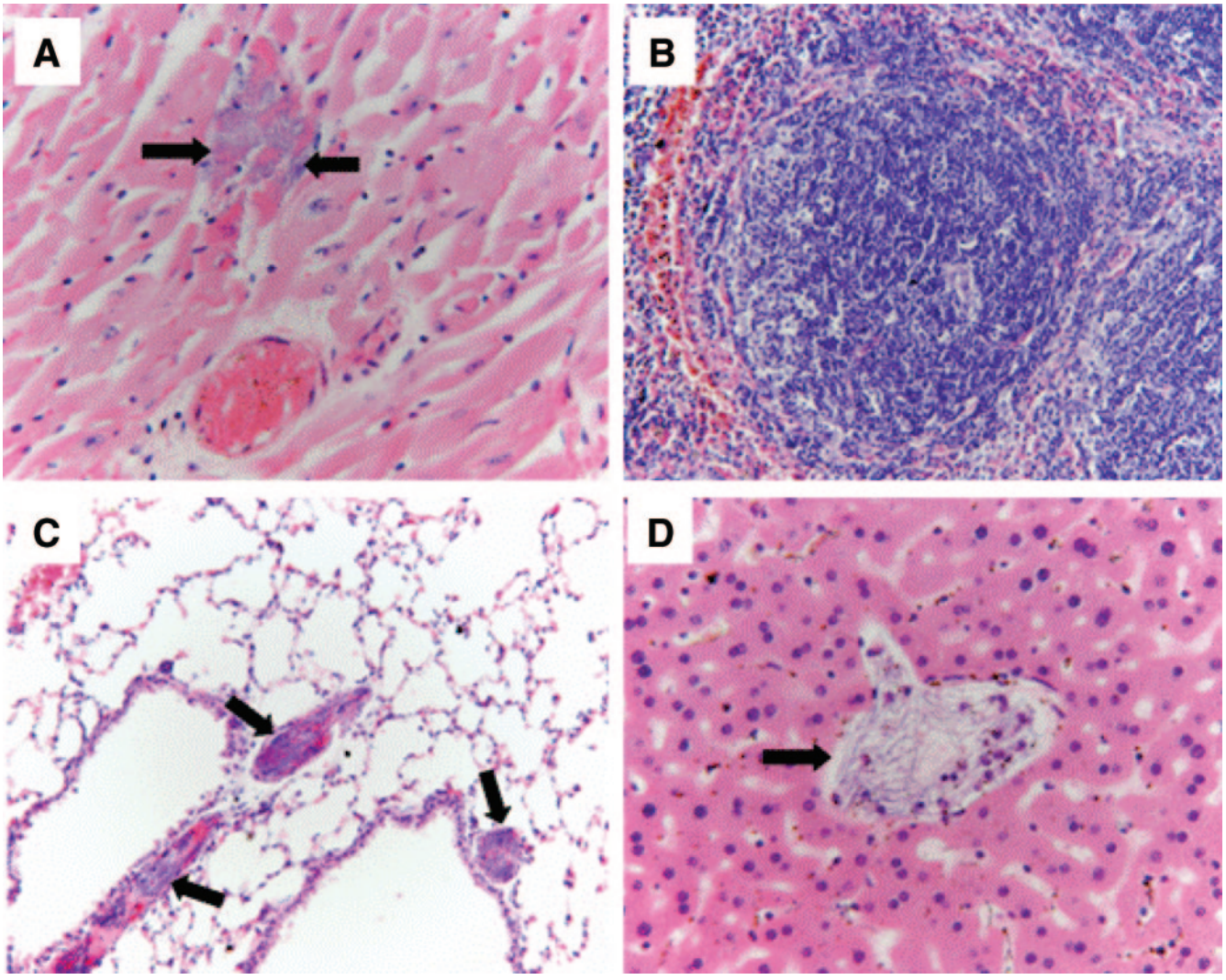

FIG. 6. Representative light photomicrographs of hematoxylin- and eosin-stained tissues collected from moribund A/J mice challenged with aerosolized *B. anthracis* Sterne spores. Arrows indicate bacteria. Original magnification is specified for each panel. (A) Heart muscle section. Note clusters of bacilli in myocardium and absence of inflammation. Magnification, ×400. (B) Spleen section demonstrating lymphocyte depletion in white pulp. Magnification, ×200. (C) Lung section with bacilli in vessels. Magnification, ×200. (D) Liver section with bacilli in a central vein. Magnification, ×400.

has been described in other animal models, and the need for high-containment facilities and use of a select agent are eliminated.

Inhalational anthrax is the most deadly form of the disease, resulting in a high mortality rate after exposure. Although other methods of spore inoculation have been used for studying inhalational *B. anthracis* pathogenesis, including i.n. and i.t. instillation, the current study used exposure to aerosols for anthrax infection. The aerosol exposure method is preferable to other methods of pulmonary introduction because exposure to aerosols results in a uniform distribution of inhaled particles throughout the lung, whereas i.t. or i.n. inoculation results in a nonuniform distribution (1, 3, 19, 35, 41). The dispersal of *B. anthracis* spores in the lungs after challenge by the various routes of pulmonary exposure may impact disease progression because it can affect the ability of the macrophage to control bacilli outgrowth. Alveolar macrophages are the primary cell to phagocytose *B. anthracis* spores during pulmonary infection, and once the spore germinates inside the cell, the macrophage can kill vegetative cells (23) and control disease progression. As macrophage uptake is affected by the route of administration (7) and the number of spores engulfed by a single alveolar macrophage has a significant effect on bacilli replication and macrophage survival (39), selecting the appropriate mechanism of spore administration used for the study of inhalational *B. anthracis* pathogenesis is important. Following aerosol delivery, spores are dispersed evenly throughout the lung, and a large number of macrophages are involved in controlling infection by engulfing spores and killing vegetative bacilli. However, an identical inoculum delivered by a method resulting in the nonuniform dispersal of spores (e.g., i.t. or i.n.) throughout the lung may alter disease progression because the number of spores engulfed by individual macrophages would be greater, and the probability of bacteria overcoming macrophage de-

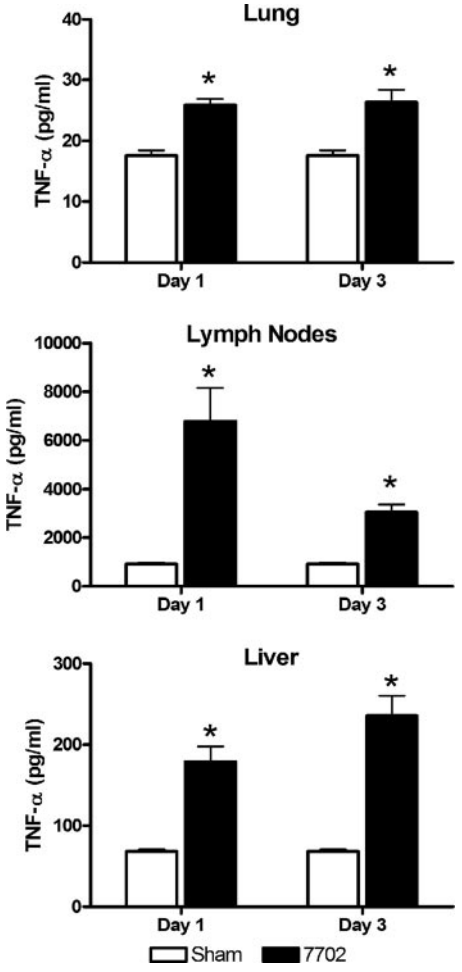

FIG. 7. TNF-α levels in lungs, lymph nodes, and livers of mice after aerosol challenge with *B. anthracis* Sterne spores. Groups of A/J mice were exposed to aerosols of spores with an average pulmonary retained dose of 3×10^6 spores per mouse. Tissue homogenates were collected at days 1 or 3 postchallenge and assayed for TNF-α by enzyme-linked immunosorbent assay. Lungs, lymph nodes, and livers from challenged (filled bars) or control mice (open bars) were pooled for each data point (n), and the graph shows mean ± standard error of the mean for $n = 5$ on day 1 and $n = 3$ on day 3. A Student's t test was used for statistical analysis, and P values of <0.05 are indicated by an asterisk.

fenses would be higher (39). Different pulmonary administration routes (i.t and i.n. versus aerosol exposure) can vary the course or kinetics of the host response, subsequently altering disease pathogenesis (31, 32, 42). As pulmonary anthrax after exposure to spore aerosols is the most likely route of infection to be used in any future biowarfare or bioterrorist attack, the aerosol delivery system is preferred for modeling inhalational anthrax and studying host pathogen interactions.

In order to compare the pathology observed in other animal models of inhalational *B. anthracis* to that of mice in the current study, five moribund mice challenged with Sterne spores were sacrificed, and hematoxylin- and eosin-stained sections of the lungs, liver, spleen, and heart were examined microscopically. The observations made from moribund mice were compared to previous reports detailing pathology in rabbits (51), rhesus monkeys (12), and cynomolgus macaques (44). In mice, bacteria were generally present in one or more organs, with the heart, liver, and lungs being more frequently colonized than the spleen. In most instances bacteria were observed within blood vessels with little to no inflammatory response, suggesting fulminate bacteremia. Although inhalation anthrax symptoms in humans frequently include pneumonia with pleural effusions and hemorrhagic mediastinitis, pneumonia is less common in several animal models, specifically, in rabbits and macaques, which have previously been established as viable inhalation anthrax models (44, 51). The lower incidence of pneumonia in these animal models may be due to the relative absence of preexisting lung conditions in laboratory animals (versus humans), as was suggested previously by Zaucha et al., and may extend to laboratory mice in particular, due to the use of healthy mice with typically pristine lungs (51).

In our study, two out of five mice exposed to aerosolized *B. anthracis* exhibited clusters of bacteria within pulmonary blood vessels in the absence of an inflammatory response. Pulmonary hemorrhages were observed in two mice, with occasional attenuation of airway epithelium. One mouse presented with extensive pulmonary lesions which were primarily regions of hemorrhage with necrosis and consolidation. Similar findings were noted in an inhalation anthrax model using cynomolgus macaques, as 100% of non-human primate lung sections showed hemorrhages (44). Vegetative *B. anthracis* bacilli were apparent in 79% of lungs, while congestion (64%), edema (50%), and inflammation (29%) were also noted in many of the affected macaques. In a rhesus monkey model of inhalation anthrax, 15% of infected animals showed anthrax-related pneumonia with mild neutrophilic infiltrates and bacilli in the alveoli. Alveolar hemorrhages were observed in 31% of monkeys (12). Bacterial loads in the lungs of moribund mice varied, with most animals exhibiting changes in lung CFU values with heat treatment, indicating the presence of vegetative bacilli in the lungs of most of these animals. Interestingly, although the total number of CFU in the lungs of moribund mice was high, the number of heat-resistant CFU (spores) was not reduced relative to day 1 (Fig. 2 and 5). This observation suggests that the increase in the lung CFU counts in moribund mice is due to the presence of vegetative bacilli in the pulmonary vasculature. This finding is consistent with histological changes in the lungs, as bacilli were present in the vessels of most moribund mice. As it is difficult to determine the time at which bacteremia occurs, some mice may exhibit signs of death early after bacterial dissemination, whereas others may not become moribund until the systemic bacterial load is extremely high (10^8 CFU) and the pathology more severe. Mice typically exhibit moribund symptoms for up to 12 h, and the length of time animals displayed these symptoms before being identified and euthanized for tissue collection were likely different. This may help to explain pathological differences observed between moribund mice.

The liver histopathology observed in cynomolgus macaques challenged with fully virulent anthrax were similar to those seen in mice in this study, with 71% of macaques and 60% (3/5) of mice exhibiting bacteria in hepatic sinusoids and with 30% of the macaques and 20% (1/5) of the mice displaying hepatic necrosis. However, acute inflammation (leukocytosis) was apparent in nearly all cynomolgus monkey livers, which was not observed in the mice. Interestingly, the most common hepatic

finding in the rhesus model was Ito cell hypertrophy (6 of 13 monkeys), which has not been reported in any other animal model, nor was it noted in our mice.

Other hepatic findings in rhesus macaques were foci of hepatocellular degeneration and necrosis in 23% of monkeys (3/13), which was similar to findings reported in other animal models, and acute hepatitis, which was present in 23% of rhesus monkeys. Focal hepatic necrosis was present in one out of five moribund mice in the current study. Specific hepatic findings were not reported in the rabbit model (51). The differences between the hepatic findings observed in mice in the current study and other animal models may be due to the sensitivity of A/J mice to anthrax infection, as these mice do not survive long enough to mount a strong, inflammatory immune response. Though TNF-α levels were elevated in the liver early after infection, the levels were only twofold higher than in uninfected animals. In addition, the bacterial loads in the livers of moribund mice were substantially higher than loads in mice on days 1 and 3 after challenge, in which TNF-α levels were measured. Taken together, early bacterial loads in the liver of mice may not induce a robust proinflammatory cytokine response that results in the infiltration of inflammatory cells, which likely explains the differences in acute inflammation and hepatic pathology observed in other animal models.

The splenic lesions in our mice most commonly exhibited lymphocytic depletion that was often accompanied by necrosis and occasional hemorrhage. In the rabbit model of *B. anthracis* infection, all of the rabbits exhibited an acute fibrinous splenitis (51). Rhesus monkeys showed lymphoid depletion, histiocytosis, hemorrhage, or acute splenitis with or without necrosis (12) while the spleens of cynomolgus macaques had suppurative inflammation and fibrin (44). Through the first 5 days of infection in mice, on average, less than 40% of challenged mice had CFU in the spleen, and those that were culture positive had relatively low CFU counts (5.1×10^4). However, nearly all moribund mice had approximately 10^6 CFU in the spleen, indicating bacterial dissemination at the end stages of disease. The large bacterial burden in the spleen of moribund mice is likely accompanied by large toxin production by the bacteria, which may result in lymphoid depletion.

Two rhesus monkeys exhibited extensive foci of hemorrhage in the myocardium (15%), and acute myocarditis was found in one of the monkeys (12). Cynomolgus monkeys showed myocardial hemorrhages (29%) and inflammation (29%) (44). In our mouse model, four out of five mice (80%) had bacteria present in the vessels or myocardium with little to no inflammatory response. Histopathological findings were not specifically reported for the heart in the rabbit model although the authors noted that bacilli were observed within the vasculature of nearly all tissues examined (51).

Similarities in disease progression and lesions in mice challenged with aerosolized Sterne spores compared to rabbit and cynomolgus or rhesus macaques challenged with fully virulent spores suggest that the mouse is a valuable model of inhalation anthrax. Using an aerosol challenge will allow for characterization of immune responses in the lungs and lymph nodes of infected animals that is most relevant to inhalational anthrax. Dissemination of *B. anthracis* after inhalation of spores is suggested to occur after spores are phagocytosed by APCs in the lung and transported to the draining lymph nodes (15, 29, 38). During this time, germination and vegetative outgrowth occur in the cell. Data from the current study concur with previous findings and show that spores do not germinate in the lung, but spores and vegetative bacilli can be found in the draining lymph nodes within a day of infection. In addition, even 5 days after challenge, minimal pathology in the lung was observed. Only when bacteria have disseminated throughout the body and vegetative bacilli return to the lungs, as seen in moribund mice, are histological changes observed in the lungs. Together, these data indicate that the lungs serve as a mucosal port of entry, but the germination and outgrowth of spores in the pulmonary draining lymph nodes are likely the primary sites of activation of the host immune response after pathogen recognition.

The utility and application of the described murine aerosol challenge model was used to investigate in vivo cytokine responses after inhalation of spores. TNF-α is a potent proinflammatory cytokine produced after host recognition of invading microbes by innate Toll-like receptors. Although TNF-α is primarily produced by macrophages, it can also be secreted by lymphoid and endothelial cells. TNF-α stimulates endothelial cells to produce proteins that alter vascular permeability in an attempt to control microbial spread into the bloodstream. In addition, TNF-α can stimulate the maturation and subsequent migration of dendritic cells to the draining lymph nodes. TNF-α has a role in controlling intracellular and extracellular microbial pathogens, as TNF-knockout mice exhibit heightened sensitivity after challenge with *Mycobacterium tuberculosis* (9), *Listeria monocytogenes* (45), or *Leishmania* (37). Following inhalational *B. anthracis* challenge, the draining lymph nodes showed a marked increase in TNF-α 1 day after challenge; however, these levels decreased by day 3. TNF-α may play a role in inducing the migration of infected APCs to the draining lymph nodes early after challenge. It has previously been shown that murine macrophages infected with *B. anthracis* spores produce TNF-α (34). However, as the bacteria replicate and begin producing toxins, the toxins may block TNF-α production by blocking mitogen-activated protein kinase kinase signaling (13). These data, in conjunction with data that show the presence of both spores and vegetative bacilli in the lymph nodes of challenged animals, suggest that lymph node TNF-α levels decrease at nearly the same time bacterial burdens in distal organs (liver and spleen) increase. Normally, TNF-α is involved in controlling disease progression, and *B. anthracis* toxins may block proinflammatory cytokine production in the lymph nodes which allows for bacterial dissemination (13). Further studies are warranted to investigate TNF-α levels in moribund mice, as well as levels of other proinflammatory cytokines, such as interleukin-1 and interleukin-6, which have shown to be increased in primary cells infected with spores (33, 34).

This report summarizes the course of inhalational anthrax disease in mice after aerosol exposure and demonstrates that the murine aerosol challenge model is both relevant and useful for the study of *B. anthracis* pathogenesis. The course of anthrax disease in complement-deficient mice (A/J) challenged with aerosolized Sterne spores ($pX01^+$ $pX02^-$) is similar to that observed in other animal species (rabbits, guinea pigs, and non-human primates) challenged

with fully virulent *B. anthracis*, as bacterial dissemination and pathological changes observed in mice were similar in comparison. We were able to use the aerosol challenge model to show changes in TNF-α levels in lungs, liver, and lymph nodes during the early stages of disease. This challenge model will be valuable in understanding inhalational *B. anthracis* pathogenesis and identifying components of the host immune system required for bacterial clearance and survival after aerosol infection. In addition, it can serve as a model for screening a new generation of vaccines and postexposure therapeutics.

ACKNOWLEDGMENTS

We thank Karen Meysick and Manuel Osorio for critical reading of the manuscript.

This work was supported by National Institutes of Health, National Institute of Allergy and Infectious Diseases, grant U54 AI50804, Mid-Atlantic Regional Center of Excellence in Biodefense Research.

REFERENCES

1. **Bakker-Woudenberg, I. A.** 2003. Experimental models of pulmonary infection. J. Microbiol. Methods **54:**295–313.
2. **Barnes, J. M.** 1947. The development of anthrax following administration of spores by inhalation. Br. J. Exp. Pathol. **28:**385–394.
3. **Brain, J. D., D. E. Knudson, S. P. Sorokin, and M. A. Davis.** 1976. Pulmonary distribution of particles given by intratracheal instillation or by aerosol inhalation. Environ. Res. **11:**13–33.
4. **Brittingham, K. C., G. Ruthel, R. G. Panchal, C. L. Fuller, W. J. Ribot, T. A. Hoover, H. A. Young, A. O. Anderson, and S. Bavari.** 2005. Dendritic cells endocytose *Bacillus anthracis* spores: implications for anthrax pathogenesis. J. Immunol. **174:**5545–5552.
5. **Dalldorf, F. G., A. F. Kaufmann, and P. S. Brachman.** 1971. Woolsorter's disease. Arch. Pathol. **92:**418–426.
6. **Dixon, T. C., A. A. Fadl, T. M. Koehler, J. A. Swanson, and P. C. Hanna.** 2000. Early *Bacillus anthracis*-macrophage interactions: intracellular survival and escape. Cell Microbiol. **2:**453–463.
7. **Dorries, A. M., and P. A. Valberg.** 1992. Heterogeneity of phagocytosis for inhaled versus instilled material. Am. Rev. Respir. Dis. **146:**831–837.
8. **Finlay, W. J. J., N. A. Logan, and A. D. Sutherland.** 2002. *Bacillus cereus* emetic toxin production in cooked rice. Food Microbiol. **19:**431–439.
9. **Flynn, J. L., M. M. Goldstein, J. Chan, K. J. Triebold, K. Pfeffer, C. J. Lowenstein, R. Schreiber, T. W. Mak, and B. R. Bloom.** 1995. Tumor necrosis factor-alpha is required in the protective immune response against *Mycobacterium tuberculosis* in mice. Immunity **2:**561–572.
10. **Fouet, A., and S. Mesnage.** 2002. *Bacillus anthracis* cell envelope components. Curr. Top. Microbiol. Immunol. **271:**87–113.
11. **Friedlander, A. M., S. L. Welkos, M. L. M. Pitt, J. W. Ezzell, P. L. Worsham, K. J. Rose, B. E. Ivins, J. R. Lowe, G. B. Howe, P. Mikesell, and W. B. Lawrence.** 1993. Postexposure prophylaxis against experimental inhalation anthrax. J. Infect. Dis. **167:**1239–1243.
12. **Fritz, D. L., N. K. Jaax, W. B. Lawrence, K. J. Davis, M. L. Pitt, J. W. Ezzell, and A. M. Friedlander.** 1995. Pathology of experimental inhalation anthrax in the rhesus monkey. Lab. Investig. **73:**691–702.
13. **Fukao, T.** 2004. Immune system paralysis by anthrax lethal toxin: the roles of innate and adaptive immunity. Lancet Infect. Dis. **4:**166–170.
14. **Greenberger, M. J., R. M. Strieter, S. L. Kunkel, J. M. Danforth, R. E. Goodman, and T. J. Standiford.** 1995. Neutralization of IL-10 increases survival in a murine model of *Klebsiella pneumonia*. J. Immunol. **155:**722–729.
15. **Guidi-Rontani, C.** 2002. The alveolar macrophage: the Trojan horse of *Bacillus anthracis*. Trends Microbiol. **10:**405–409.
16. **Guidi-Rontani, C., M. Levy, H. Ohayon, and M. Mock.** 2002. Fate of germinated *Bacillus anthracis* spores in primary murine macrophages. Mol. Microbiol. **42:**931–938.
17. **Guidi-Rontani, C., Y. Pereira, S. Ruffie, J. C. Sirard, M. Weber-Levy, and M. Mock.** 1999. Identification and characterization of a germination operon on the virulence plasmid pXO1 of *Bacillus anthracis*. Mol. Microbiol. **33:**407–414.
18. **Guidi-Rontani, C., M. Weber-Levy, E. Labruyere, and M. Mock.** 1999. Germination of *Bacillus anthracis* spores within alveolar macrophages. Mol. Microbiol. **31:**9–17.
19. **Halperin, S. A., S. A. Heifetz, and A. Kasina.** 1988. Experimental respiratory infection with *Bordetella pertussis* in mice: comparison of two methods. Clin. Investig. Med. **11:**297–303.
20. **Harvill, E. T., G. Lee, V. K. Grippe, and T. J. Merkel.** 2005. Complement depletion renders C57BL/6 mice sensitive to the *Bacillus anthracis* Sterne strain. Infect. Immun. **73:**4420–4422.
21. **Heninger, S., M. Drysdale, J. Lovchik, J. Hutt, M. F. Lipscomb, T. M. Koehler, and C. R. Lyons.** 2006. Toxin-deficient mutants of *Bacillus anthracis* are lethal in a murine model for pulmonary anthrax. Infect. Immun. **74:**6067–6074.
22. **Ireland, J. A., and P. C. Hanna.** 2002. Macrophage-enhanced germination of *Bacillus anthracis* endospores requires *gerS*. Infect. Immun. **70:**5870–5872.
23. **Kang, T. J., M. J. Fenton, M. A. Weiner, S. Hibbs, S. Basu, L. Baillie, and A. S. Cross.** 2005. Murine macrophages kill the vegetative form of *Bacillus anthracis*. Infect. Immun. **73:**7495–7501.
24. **Klein, F., J. S. Walker, D. F. Fitzpatrick, R. E. Lincoln, B. G. Mahlandt, W. I. J. Jones, J. P. Dobbs, and K. J. Hendrix.** 1966. Pathophysiology of anthrax. J. Infect. Dis. **116:**123–138.
25. **Koch, R.** 1876. Die etiologie der milzbrand krankheit hegrundet auf die entwickelungsgeschichte des *Bacillus anthracis*. Beitr. Biol. Pflanz. **2:**277–283.
26. **Lacy, D. B., and R. J. Collier.** 2002. Structure and function of anthrax toxin. Curr. Top. Microbiol. Immunol. **271:**61–85.
27. **LaForce, F. M., F. H. Bumford, J. C. Feeley, S. L. Stokes, and D. B. Snow.** 1969. Epidemiologic study of a fatal case of inhalation anthrax. Arch. Environ. Health **18:**798–805.
28. **Lincoln, R. E., D. R. Hodges, F. Klein, B. G. Mahlandt, W. I. J. Jones, B. W. Haines, R. M. A., and J. S. Walker.** 1965. Role of lymphatics in the pathogenesis of anthrax. J. Infect. Dis. **115:**481–494.
29. **Lyons, C. R., J. Lovchik, J. Hutt, M. F. Lipscomb, E. Wang, S. Heninger, L. Berliba, and K. Garrison.** 2004. Murine model of pulmonary anthrax: kinetics of dissemination, histopathology, and mouse strain susceptibility. Infect. Immun. **72:**4801–4809.
30. **Mock, M., and A. Fouet.** 2001. Anthrax. Annu. Rev. Microbiol. **55:**647–671.
31. **Osier, M., R. B. Baggs, and G. Oberdorster.** 1997. Intratracheal instillation versus intratracheal inhalation: influence of cytokines on inflammatory response. Environ. Health Perspect. **105**(Suppl. 5)**:**1265–1271.
32. **Osier, M., and G. Oberdorster.** 1997. Intratracheal inhalation vs intratracheal instillation: differences in particle effects. Fundam. Appl. Toxicol. **40:**220–227.
33. **Pickering, A. K., and T. J. Merkel.** 2004. Macrophages release tumor necrosis factor alpha and interleukin-12 in response to intracellular *Bacillus anthracis* spores. Infect. Immun. **72:**3069–3072.
34. **Pickering, A. K., M. Osorio, G. M. Lee, V. K. Grippe, M. Bray, and T. J. Merkel.** 2004. Cytokine response to infection with *Bacillus anthracis* spores. Infect. Immun. **72:**6382–6389.
35. **Pritchard, J. N., A. Holmes, J. C. Evans, N. Evans, R. J. Evans, and A. Morgan.** 1985. The distribution of dust in the rat lung following administration by inhalation and by single intratracheal instillation. Environ. Res. **36:**268–297.
36. **Reed, L. J., and H. Muench.** 1938. A simple method of estimating fifty percent endpoints. Amer. J. Hyg. **27:**493–497.
37. **Ritter, U., J. Mattner, J. S. Rocha, C. Bogdan, and H. Korner.** 2004. The control of *Leishmania* (Leishmania) *major* by TNF in vivo is dependent on the parasite strain. Microbes Infect. **6:**559–565.
38. **Ross, J. M.** 1957. The pathogenesis of anthrax following the administration of spores by the respiratory route. J. Pathol. Bacteriol. **73:**485–494.
39. **Ruthel, G., W. J. Ribot, S. Bavari, and T. A. Hoover.** 2004. Time-lapse confocal imaging of development of *Bacillus anthracis* in macrophages. J. Infect. Dis. **189:**1313–1316.
40. **Shafa, F., B. J. Moberly, and P. Gerhardt.** 1966. Cytological features of anthrax spores phagocytized in vitro by rabbit alveolar macrophages. J. Infect. Dis. **116:**401–413.
41. **Steinbach, W. J., D. K. Benjamin, Jr., S. A. Trasi, J. L. Miller, W. A. Schell, A. K. Zaas, W. M. Foster, and J. R. Perfect.** 2004. Value of an inhalational model of invasive aspergillosis. Med. Mycol. **42:**417–425.
42. **Tang, C. M., J. Cohen, T. Krausz, S. Van Noorden, and D. W. Holden.** 1993. The alkaline protease of *Aspergillus fumigatus* is not a virulence determinant in two murine models of invasive pulmonary aspergillosis. Infect. Immun. **61:**1650–1656.
43. **Turnbull, P. C.** 2002. Introduction: anthrax history, disease and ecology. Curr. Top. Microbiol. Immunol. **271:**1–19.
44. **Vasconcelos, D., R. Barnewall, M. Babin, R. Hunt, J. Estep, C. Nielsen, R. Carnes, and J. Carney.** 2003. Pathology of inhalation anthrax in cynomolgus monkeys (*Macaca fascicularis*). Lab. Investig. **83:**1201–1209.
45. **Virna, S., M. Deckert, S. Lutjen, S. Soltek, K. E. Foulds, H. Shen, H. Korner, J. D. Sedgwick, and D. Schluter.** 2006. TNF is important for pathogen control and limits brain damage in murine cerebral listeriosis. J. Immunol. **177:**3972–3982.
46. **Welkos, S. L.** 1991. Plasmid-associated virulence factors of non-toxigenic (pX01$^-$) *Bacillus anthracis*. Microb. Pathog. **10:**183–198.
47. **Welkos, S. L., and A. M. Friedlander.** 1988. Comparative safety and efficacy against *Bacillus anthracis* of protective antigen and live vaccines in mice. Microb. Pathog. **5:**127–139.

48. **Welkos, S. L., and A. M. Friedlander.** 1988. Pathogenesis and genetic control of resistance to the Sterne strain of *Bacillus anthracis*. Microb. Pathog. **4:**53–69.
49. **Welkos, S. L., T. J. Keener, and P. H. Gibbs.** 1986. Differences in susceptibility of inbred mice to *Bacillus anthracis*. Infect. Immun. **51:**795–800.
50. **Welkos, S. L., N. J. Vietri, and P. H. Gibbs.** 1993. Non-toxigenic derivatives of the Ames strain of *Bacillus anthracis* are fully virulent for mice: role of plasmid pX02 and chromosome in strain-dependent virulence. Microb. Pathog. **14:**381–388.
51. **Zaucha, G. M., L. M. Pitt, J. Estep, B. E. Ivins, and A. M. Friedlander.** 1998. The pathology of experimental anthrax in rabbits exposed by inhalation and subcutaneous inoculation. Arch. Pathol. Lab. Med. **122:**982–992.

Editor: V. J. DiRita